Actively Controlled Adaptive Shape Memory Alloy Based Smart Blades for Wind Turbines

A PROJECT REPORT

Submitted in partial fulfilment of the requirements for the award of the degrees

of
BACHELOR OF TECHNOLOGY
in

MECHANICAL ENGINEERING

Submitted by:
Akarsh Jain (130003004)
Ezaj Ahmed (130003014)
Samyak Jain (130003033)

Guided by:
Dr. I. A. Palani
Dr. M. Anbarasu

INDIAN INSTITUTE OF TECHNOLOGY INDORE
December 2016

Preface

This report on “Actively Controlled Adaptive Shape Memory Alloy Based Smart Blades for Wind Turbines" is prepared under the guidance of Dr. I. A. Palani and Dr. M. Anbarasu.

Through this report we have tried to give a detailed design of smart composite wind turbine blade model embedded with prestrained nitinol wire actuators.

We have tried to the best of our abilities and knowledge to explain the content in a lucid manner with the help of CFD analysis in ANSYS. We have also added 3-D models and figures to make it more illustrative.

Akarsh Jain (130003004)
Ezaj Ahmed (130003014)
Samyak Jain (130003033)
B.Tech. IV Year
Discipline of Mechanical Engineering
IIT Indore

Acknowledgements

We would like to thank **Dr. I. A. Palani** and **Dr. M. Anbarasu** for their kind support and valuable guidance.

In addition, we would also like to acknowledge **Mr. S.S. Mani Prabu** and **Mr. Vijay Choyal** for their sincere support.

It is their help and support, due to which we became able to complete the design and technical report.

Without their support this report would not have been possible.

Akarsh Jain (130003004)
Ezaj Ahmed (130003014)
Samyak Jain (130003033)
B.Tech. IV Year
Discipline of Mechanical Engineering
IIT Indore

ABSTRACT

The change in wind flow characteristics with time will induce undesirable aerodynamic loads on rigid aerodynamic surfaces and also produce fluctuating power from the generator. Adaptive Trailing Edge provides an improved lift–drag ratio which will result in maximum but nearly constant wind energy capture. In addition to better wind energy capture adaptive trailing edge will also reduce the gust loads which induce undesirable aerodynamic loads on rigid aerodynamic surfaces. With flexible smart structures, deflections can be easily attained by embedding smart materials such as SMA, piezoelectric materials, dielectric elastomers etc. Active shape control by smart materials embedded structures is an effective choice for adaptive blade because these structures are simple in design, light weight, no moving parts and scalable. Recent developments in SMA hybrid structures are gaining momentum due to its high energy density and high strain recovery.

An experimental study has been conducted to design and fabricate smart composite wind turbine blade model embedded with prestrained nitinol wire actuators. The blade is developed with 4 parallel prestrained wires eccentrically embedded in Glass/epoxy host and cured successfully. Another blade is developed using SMA spring fixed to the edges of Glass/epoxy blade. Multi-cycle thermomechanical bending actuations of blades are performed experimentally by applying various levels of electric current to the SMA (both wires and springs). The performance characteristics showed that the end deflections of up to 20.9 mm with the spring and 13.1 mm with the wires were achieved from smart glass/epoxy blades.

Keywords

- Smart structures
- Ni-Ti
- Shape memory alloy
- Trailing edge
- CFD analysis

Table of Contents

LIST OF FIGURES

CHAPTER 1: INTRODUCTION

1.1 WIND TURBINE

A wind turbine obtains its power input by converting the force of the wind into a torque acting on the rotor blades. The amount of energy which the wind transfers to the rotor depends on the density of the air, the rotor area, and the wind speed. The blades have a special curved shape, similar to the **AIRFOIL** wings on a plane. When wind blows past a plane's wings, it moves them upward with a force termed as lift; when it blows past a turbine's blades, it spins them around instead.

Wind turbines can be separated into two basic types determined by which way the turbine spins. Wind turbines that rotate around a horizontal axis are more common, while vertical axis wind turbines are less frequently used.

- **Horizontal Axis Wind Turbines (HAWT)**

Figure 1 Horizontal Axis Wind Turbine [A]

A HAWT has a similar design to a windmill .the axis of blade rotation is parallel to the ground and is also parallel to the wind flow. Main advantage of HAWT is that the tall tower base allows access to stronger wind in sites with wind shear. It has higher efficiency, since the blades always move perpendicularly to the wind, receiving power through the whole rotation. In contrast, all vertical axis wind turbines involve various types of reciprocating actions which leads to inherently lower efficiency.

Whereas some of the disadvantages include Massive tower construction to support the heavy blades, gearbox, and generator and also the Components of a horizontal axis wind turbine (gearbox, rotor shaft, and brake assembly) has to be lifted into position. HAWTs require an additional yaw control mechanism to turn the blades toward the wind. HAWTs generally require a braking or yawing device in high winds to stop the turbine from spinning and destroying or damaging itself.

- **Vertical Axis Wind Turbines (VAWT)**

Figure 2 Vertical Axis Wind Turbine [A]

They have the main rotor shaft arranged vertically. The main advantage of this arrangement is that the wind turbine does not need to be pointed into the wind. With a vertical axis, the generator and other primary components can be placed near the ground, so the tower does not need to support it.

The main drawback of a VAWT generally create drag when rotating into the wind. It is difficult to mount vertical-axis turbines on towers, meaning they are often installed nearer to the base on which they rest, such as the ground or a building rooftop. The wind speed is slower at a lower altitude, so less wind energy is available for a given size turbine.

1.2 COMPONENTS OF WIND TURBINE

- The **nacelle** contains the key components of the wind turbine, including the gearbox, and the electrical generator.
- Blades and hub together form the **rotor**. The rotor blades capture the wind and transfer its power to the rotor hub.
- The **low speed shaft** of the wind turbine connects the rotor hub to the gearbox.

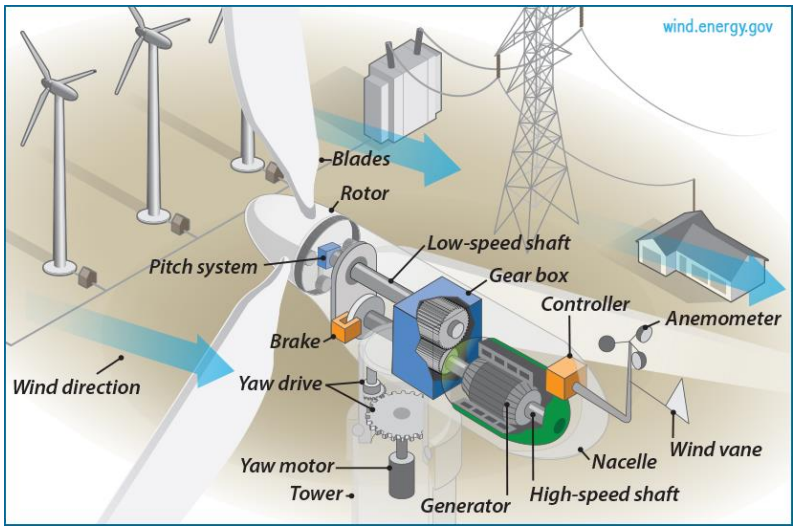

Figure 3 Components of Wind Turbine [A]

- The **gearbox** has the low speed shaft to the left. It makes the **high speed shaft** to the right turn approximately 50 times faster than the low speed shaft.
- The high speed shaft rotates and drives the **electrical generator**. It is equipped with an emergency **mechanical disc brake**.
- The electrical generator is usually a so-called induction generator or asynchronous generator.
- The **yaw mechanism** uses electrical motors to turn the nacelle with the rotor against the wind. It orients upwind turbines to keep them facing the wind when the direction changes.
- The **anemometer and the wind wane** are used to measure the speed and the direction of the wind respectively.
- **Tower** is made from tubular steel, concrete, or steel lattice and supports the structure of the turbine. Because wind speed increases with height, taller towers enable turbines to capture more energy and generate more electricity.

1.3 AIRFOILS

An AIRFOIL is the term used to describe the cross-sectional shape of an object that, when moved through a fluid such as air, creates an aerodynamic force. An airfoil shaped body moved through a fluid produces an aerodynamic force. The component of this force perpendicular to the direction of motion is called **Lift**. The component parallel to the direction of motion is called **Drag**.

Aerofoil Terminology

- **Leading Edge** : Forward edge of the aerofoil
- **Trailing Edge** : Aft edge of the aerofoil
- **Chord**: Line connecting the leading and trailing edge. Denotes the length of the aerofoil
- **Mean Camber Line**: Line drawn half way between the upper and lower surface of the aerofoil. Denotes the amount of curvature of the wing
- **Point of Maximum Thickness** : Thickest part of the wing expressed as a percentage of the chord

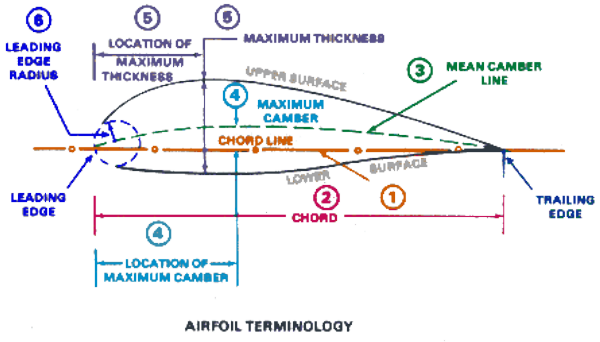

Figure 4 Airfoil Terminology [B]

The NACA airfoils are airfoil shapes developed by **the National Advisory Committee for Aeronautics (NACA)**. NACA was a U.S. federal agency founded on March 3, 1915, to promote and institutionalize aeronautical research. On October 1, 1958, the agency was dissolved, and its assets and personnel transferred to the newly created National Aeronautics and Space Administration (NASA).

4 Digit code used to describe airfoil shapes

- 1st Digit – Maximum camber in Percent chord
- 2nd Digit – Location of maximum camber along chord line (from leading edge) in tenths of chord length
- 3rd and 4rd Digits – maximum thickness in percent chord

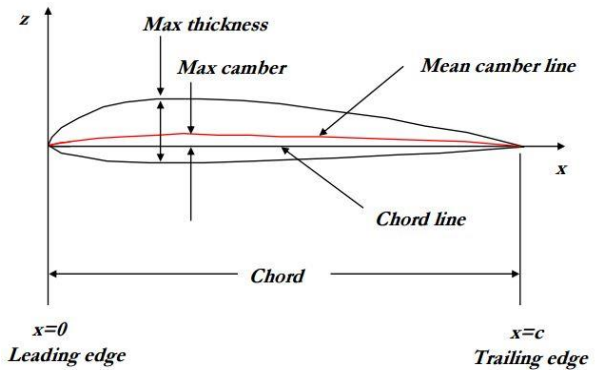

Figure 5 Airfoil Description[B]

An airfoil of the NACA 4-digit series such as the NACA 4412 (to be read as 4 - 4 - 12) describes an airfoil with a camber of 0.04 chord located at 0.40 chord, with 0.12 chord of maximum thickness.

1.4 WIND TURBINE AERODYNAMICS

The basic principle behind an aerofoil is described by Bernoulli's theorem. Basically, this states that total pressure is equal to static pressure (due to the weight of air above) plus dynamic pressure (due to the motion of air).

LIFT

The air sliding along the upper surface of the wing will move faster than on the lower surface. This means that the pressure will be lowest on the upper surface. This creates the lift, i.e. the force pulling upwards that enables the plane to fly. The lift is perpendicular to the direction of the wind.

As the angle of attack (the angle between the chord line and relative air flow) is increased, more lift is created. Once the critical angle of attack is reached (generally around 14 degrees) the aerofoil will stall.

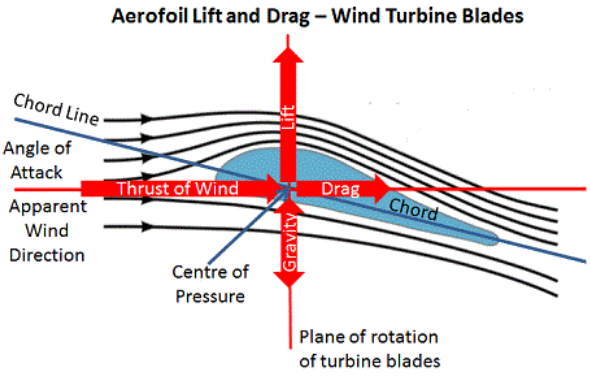

Figure 6 Lift and Drag Forces [C]

DRAG

Drag is a force acting opposite to the relative motion of any object moving with respect to a surrounding fluid. It is in the direction of fluid flow.

THE LIFT FORCE PROVIDES THE DRIVING TORQUE TO THE ROTOR.

The formula for lift (L) and the formula for drag (D) is given below:

$$C_Ł = \frac{L}{½\rho A W^2} \qquad C_D = \frac{D}{½\rho A W^2}$$

C_L : Coefficient of Lift

C_D : Coefficient of Drag

W : Relative wind as experienced by the wind turbine blade

ρ : Air Density

A : Area of the wind turbine

1.5 WIND ENERGY

Where Does Wind Energy Come From?

All renewable energy (except tidal and geothermal power), and even the energy in fossil fuels, ultimately comes from the sun. The sun radiates 174,423,000,000,000 kilowatt hours of energy to the earth per hour. In other words, the earth receives 1.74 x 10^{17} watts of power [1]

About 1 to 2 per cent of the energy coming from the sun is converted into wind energy. That is about 50 to 100 times more than the energy converted into biomass by all plants on earth.

Factors Affecting Wind Motion

Since pressure differences are mainly **caused by unequal heating of the earth's surface**, solar radiation may be called the ultimate driving force of the wind. If the earth were stationary and had a uniform surface, air would flow directly from high pressure areas to low pressure areas. Because none of these conditions exist, the direction and speed of wind are controlled by a number of factors such as:

- **Pressure Gradient Force:** This is the force generated due to the differences in horizontal pressure, and it operates from the high pressure area to a low pressure area. The wind direction follows the direction of change of pressure, i.e. perpendicular to the isobars.
- **Coriolis force:** Due to the earth's rotation, winds do not cross the isobars at right angles as the pressure gradient force directs, but get deflected from their original path. This deviation is the result of the earth's rotation and is called the Coriolis Effect or Coriolis force. Due to this effect, winds in the northern hemisphere get deflected to the right of their path and those in the southern hemisphere to their left. The Coriolis force changes wind direction but not its speed.
- **Centripetal Acceleration:** Due to inward acceleration of air towards the centre of rotation on the rotating earth, it is possible for the air to maintain a curved path (parallel to the isobars), about a local axis of high or low pressure. It is known as centripetal acceleration.
- **Frictional Force:** The irregularities of the earth's surface offer resistance to the wind motion in the form of friction. This force determines the angle at which air will flow across the isobars, as well as the speed at which it will move. It may also alter wind direction.

[1] Danish Wind Industry Association

1.6 POWER CONTROL OF WIND TURBINES

Wind turbines are designed to produce electrical energy as cheaply as possible. Wind turbines are therefore generally designed so that they yield maximum output at moderate wind speeds around 15 metres per second. In case of stronger winds, it is necessary to waste part of the excess energy of the wind in order to avoid damaging the wind turbine. All wind turbines are therefore designed with some sort of power control.

There are two different ways of doing this safely on modern wind turbines.

- **Pitch Controlled Wind Turbines:** On a pitch controlled wind turbine the turbine's electronic controller repeatedly checks the power output of the turbine. When the power output becomes too high, it sends an order to the blade pitch mechanism which immediately pitches (turns) the rotor blades slightly out of the wind. Conversely, the blades are turned back into the wind whenever the wind drops again. The pitch mechanism is usually operated using hydraulics.
- **Stall Controlled Wind Turbines:** Stall controlled wind turbines have the rotor blades bolted onto the hub at a fixed angle. The geometry of the rotor blade profile has been aerodynamically designed to ensure that when the wind speed becomes too high, it creates turbulence on the side of the rotor blade which is not facing the wind. This stall prevents the lifting force of the rotor blade from acting on the rotor. A rotor blade for a stall controlled wind turbine is twisted slightly as you move along its longitudinal axis. This is partly done in order to ensure that the rotor blade stalls gradually rather than abruptly when the wind speed reaches its critical value. The basic advantage of stall control is that one avoids moving parts in the rotor itself, and a complex control system. On the other hand, stall control represents a very complex aerodynamic design problem and related design challenges such as stall-induced vibrations etc.

1.7 SHAPE MEMORY ALLOYS

Shape memory is a property of select materials that have the ability to "remember" the shape given during original thermo-mechanical processing allowing the material to revert to that original shape when subjected to heat.

The three main types of shape memory alloys are the copper-zinc aluminium-nickel, copper-aluminium-nickel, and nickel-titanium (NiTi) alloys but SMA's can also be created by alloying zinc, copper, gold, and iron.

The transition from the martensite phase to the austenite phase is only dependent on temperature and stress, not time, as most phase changes are, as there is no diffusion involved. It is the reversible diffusion less transition between these two phases that results in special properties. While martensite can be formed from austenite by rapidly cooling carbon-steel, this process is not reversible, so steel does not have shape-memory properties.

Nitinol

Nickel titanium, or Nitinol, properties include the shape memory effect, super elasticity, and high damping capability. Nitinol is also promising due to high energy density, large reversible changes of mechanical and physical characteristics and most importantly the ability to generate extremely high recovery stresses.

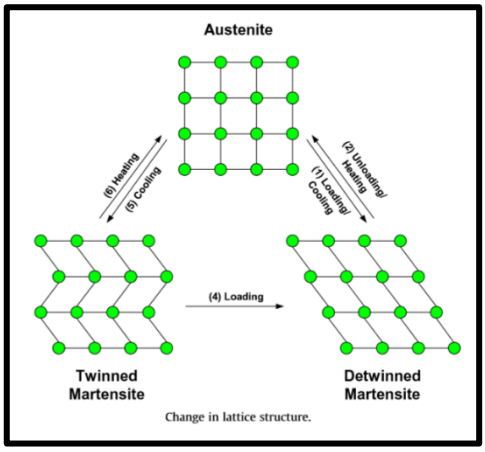

Figure 7 Phases of SMA [1]

Austenite: Nitinol's stronger, higher-temperature phase. Crystalline structure is simple cubic. Super elastic behaviour occurs in this phase (over a 50º-60ºC temperature spread)

Martensite: Nitinol's weaker, lower-temperature phase. Crystalline structure is twinned. Material is easily deformed in this phase. Once deformed in martensite, it will remain deformed until heated to austenite where it will return to its pre-deformed shape, producing the "shape memory" effect

As: temperature where material starts to transform to austenite upon heating

Af: temperature where material has finished transforming to austenite upon heating

Ms: temperature where material starts to transform to martensite upon cooling

Mf: temperature where material has finished transforming to martensite upon cooling

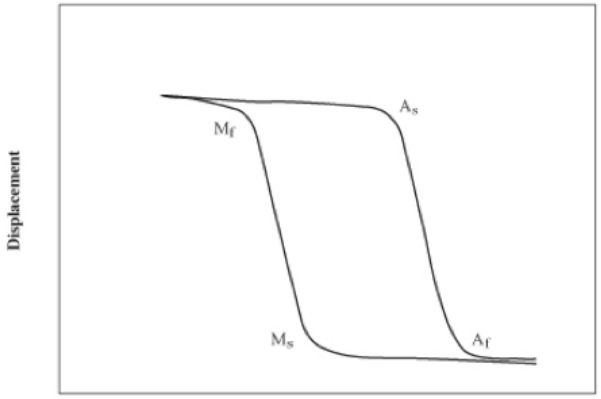

Figure 8 Transformation behaviour of Nitinol [1]

Training of Nitinol Wires

In the martensite phase, Nitinol can be bent into various shapes. To fix the "parent shape" (as it is called), the metal must be held in position and heated to about 500 ° C. The high temperature "causes the atoms to arrange themselves into the most compact and regular pattern possible" resulting in a rigid cubic arrangement known as the austenite phase (Kauffman and Mayo, 5-6). Above the transition temperature, Nitinol reverts from the martensite to the austenite phase which changes it back into its parent shape. This cycle can be repeated millions of times.

Significance of Nitinol Wires

Nitinol wires are promising due to high energy density, high damping capacity, large reversible changes of mechanical and physical characteristics and most importantly the ability to generate extremely high recovery stresses.

Present techniques uses hydraulics, servo motors etc. are heavier. Moreover, actuation with SMA can be done using less moving parts which increase the reliability.

CHAPTER 2: PROBLEM STATEMENT

The **varying wind flow characteristics with time** will induce undesirable aerodynamic loads on rigid aerodynamic surfaces**.** During the last decades, the length of wind turbine rotor blades increased to increase the swept area for higher power generation per wind turbine. Due to the longer blades, higher stresses arise, particularly at the blade root. Also as the wind turbine blades become larger and more flexible there is an increased need for locally distributed control surfaces which will reduce the requirement for the pitch control and reduce the time from actuations to load change. One way to reduce the forces acting near the blade tip region and create locally distributed control surfaces is controlling the shape of trailing edge, that is, **making the trailing edge adaptive**.

A shape morphing blade with adaptive trailing edge will change according to the wind dynamics. It will **maintain constant rotor speed and reduce fatigue load** thus **improving efficiency of the wind turbine.**

In addition, the shape change of wind turbine blades will increase the lift/drag ratio resulting in increase in lift force in comparison to drag force, when the **wind speed is below rated speed**, which in turn improves the turbine performance by better wind energy capture.

OBJECTIVES

- To configure a design for SMA embedded composite blade with optimum stiffness of the composite such that it exhibits two way shape memory effect.
- To fabricate the trained SMA wire embedded composite blade according to the design generated.
- Analyse the deflection characteristics of SMA embedded wind turbine blade.
- Compare and evaluate the performance of wind turbine having these hybrid blades with the conventional rigid blade wind turbines through CFD analysis.

CHAPTER 3: LITERATURE REVIEW

The anisotropic core flap structure presented by Stephen and Paul [2] represent a promising concept in the long-term development of adaptive control surfaces for both wind turbine and wider aerospace applications. A full-sized model of the morphing trailing edge device was manufactured and actuated in a laboratory environment. The flap consists of an aramid honeycomb core with a Carbon fibre reinforced plastic (CFRP) skin on one surface and a silicone skin on the other. The flap has integrated CFRP rods, which are connected to servo motor actuators. Many design variables were considered including skin and core materials, actuator integration and actuator spacing. The final design consisted of actuators being spaced every 250 mm in the span wise direction in order to distribute loading in the flexible structure.

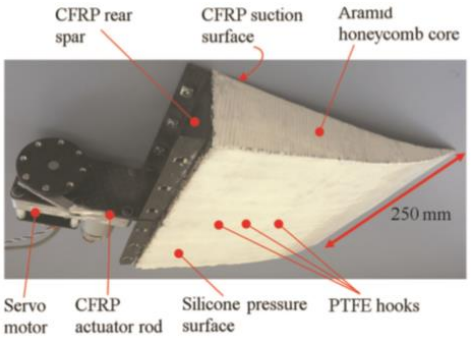

Figure 9 Morphing trailing edge design showing silicone pressure surface [2].

A woven type smart soft composite (SSC) was fabricated and implemented as a soft morphing spoiler by Min-Woo Han et al [1]. in order to adjust its aerodynamic performance by transforming its shape using a compact mechanism. The woven type SSC which consists of SMA wires for actuation and anisotropic materials to obtain directional properties were embedded together in a flexible polymeric matrix was designed for application in a trailing edge for the rear-spoiler. The structure was implemented as the trailing edge of the spoiler of a small-scale car (1 /8-scale). Also, the embedded SMA wires were divided into two different current channels to generate a bend-twist deformation intended to increase the yawing moment. To find the effects of the airflow on the generated forces by the morphing spoiler, wind tunnel tests were conducted in an open-circuit bowing-type wind tunnel. Test results showed that the proposed structure is capable of large deformations, self-recovery to its original shape, and withstanding the external forces applied through the airflow surrounding the morphing spoiler.

Figure 10 Morphing spoiler with small scale car [1]

In the work done by Hugo Rodrigue et al [3]. The smart soft composite (SSC) actuator uses pair of NiTi shape memory alloy (SMA) wires embedded in a cross-shaped polydimethylsiloxane (PDMS) matrix at constant and opposite eccentricity across the cross-section in opposite directions in order to produce a twisting motion. To evaluate the twisting performance of the cross-shaped actuator, specimens with rectangular cross-sections and cross-shaped cross-sections are made and their twist angles are measured and compared. Results show that the cross-shaped actuator is capable of a higher twisting rate by using a thinner flange due to a more stable twisting motion. Samples were built for a rectangular cross-section and a cross-shaped cross-section with varying geometry thicknesses. Results showed that the rectangular shaped actuator failed when the matrix was too thin due to large bending of the actuator. However, the cross-shaped actuator was able to remain stable for flange thicknesses as thin as 1.5 mm

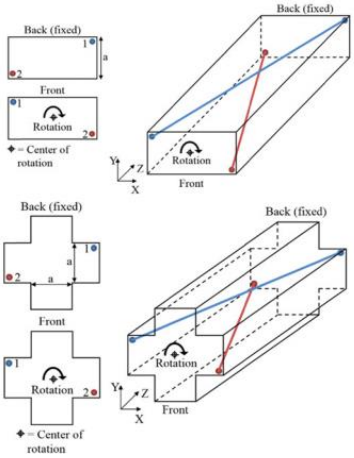

Figure 11 Configuration of the rectangular and cross-shaped twisting actuator [3].

The winglet for Unmanned aerial vehicle (UAV) was designed by Hugo Rodrigue et al[4]. for morphing its shape smoothly between the unmorphed (flat) and morphed (curved) geometries to adjust itself for optimized flight conditions by mimicking the primary wing-tip feathers of gliding birds. Winglet-shaped composite structures were fabricated, and tests were carried out with various diameters of SMA wire, numbers of embedded SMA wires, and numbers of glass-fibre fabric lamina. Furthermore, to investigate the aerodynamic forces, wind tunnel experiments were conducted with the soft morphing winglets mounted on a small-scale UAV in various angles of attack (2 deg– 13 deg). The wind tunnel tests showed that the morphed wingtip exhibited a lower drag coefficient for angles of attack greater than or equal to 4 deg and a larger lift coefficient for angles of attack greater than or equal to 9 deg. These aerodynamic forces resulted in an improvement in the L/D ratio of up to 5.8% with an angle of attack of 12 deg, using the morphed geometry indicating that aerodynamic performance of the UAV can be improved by controlling the wing tip geometry considering the inclined angle of the UAV.

Figure 12 UAV with the mounted morphing winglets Top view [4].

Shape memory materials are characterized by the ability to recover their shape after deformation under specific conditions [5]. Among the shape memory materials, shape memory alloy (SMA) materials are widely used in the design of shape memory structures due to their super elasticity, their high power to weight ratio, and also due to their shape memory effect [6].

CHAPTER 4: FABRICATION OF SMART STRUCTURES:

4.1 SMART STRUCTURES

A structure which can adapt to the changing environmental conditions is called Smart Structure. This smartness can be achieved by using smart materials like Shape-memory alloys (SMA), piezoelectric crystal, etc. SMA wires have been used to produce shape morphing effect by the Smart blades.

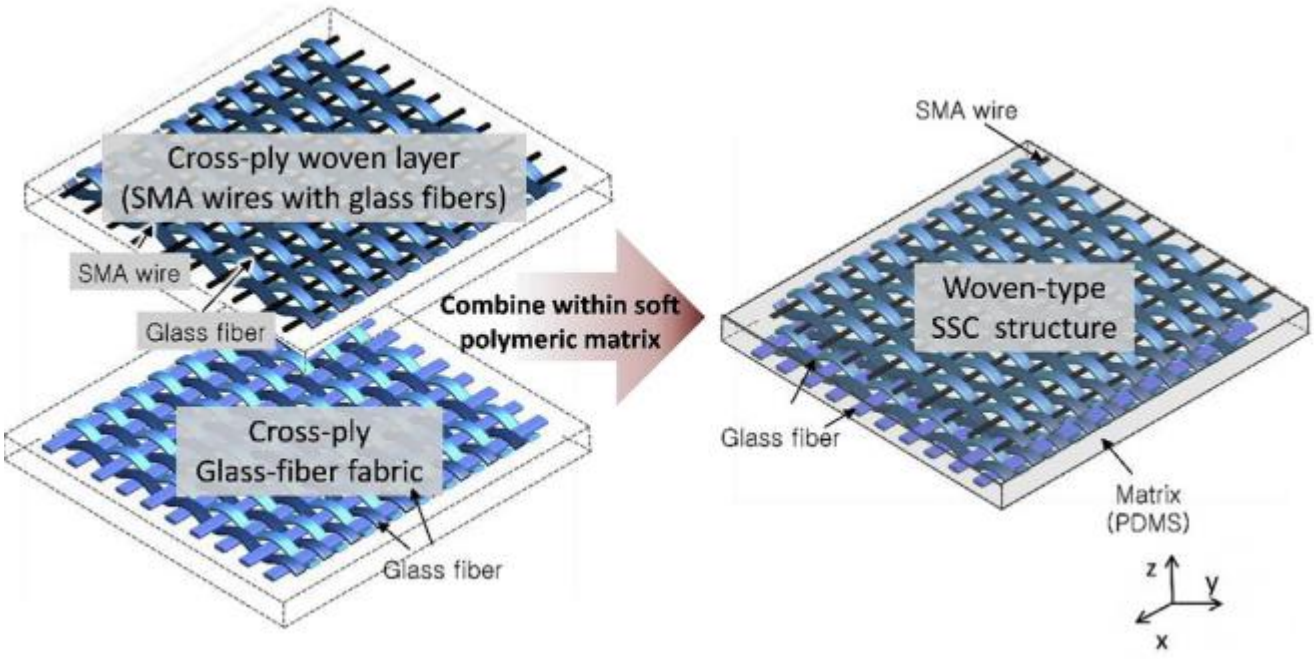

Figure 13 Woven type smart soft composite [1]

The SMA fibres are used to strengthen the matrix, to absorb strain energy and reduce the residual stress by stress-induced martensitic transformations .The embedded SMA fibres are also used to enhance the performance of structures, to improve the damping capacity, increase the impact damage resistance to minimize creep deformation, giving rise to the stiffness of the composite, for noise reduction in rotor blade systems and sound transmission/radiation of composite panels.

Two Way Shape Memory Effect

- On heating, the phase changes to austenite and the SMA changes itself to its trained shape.
- On cooling, the SMA cools down to room temperature and the inherent elasticity of the composite structure acts as a bias force and takes up the initial position.

4.2 TRAINING OF SMA WIRES

The SMA wires are trained for a particular shape in their austenitic phase. The SMA wires are heated at temperature around 500°C and trained for a particular shape at this temperature. The training can be performed by placing the wire in the fixture and heating it in either in furnace or by Joule heating.

In furnace heating, the fixture is first heated upto 700°C for 30 minutes to relieve the internal stresses. The wires are heated at 450°C for 30 minutes and then quenched in water. The process is repeated for 5 cycles.

Figure 14 Training in Muffle Furnace

Figure 15 Fixture for Training SMA

The wire can also be trained by Joule heating where the wire is placed in a fixture and 16-18 Ampere current is supplied for 5 minutes and then allowed to cool for 2 minutes. This is done for 5 cycles. However, Furnace heating is more effective than Joule heating as it shows shape remembrance property for more number of cycles.

Figure 16 Training SMA through Joules Heating

4.3 FABRICATION OF SMART STRUCTURES

A composite plate with embedded SMA wire actuators is fabricated with a polymer along with glass fibre reinforcement to provide stiffness to the blade. On heating, the SMA wire actuators can deform the composite structure and the morphing effect can be obtained. The polymers photopolymer and epoxy have been chosen on the property to get cured in the room temperature. These are light weight and can easily embed SMA wires.

Fibre Reinforced Composites

A composite material is a material made from two or more constituent materials with significantly different physical or chemical properties that, when combined, produce a material with characteristics different from the individual components.

Fibre-reinforced polymer is a composite material made of a polymer matrix reinforced with fibres. The fibres are usually glass, carbon, etc. The polymer is usually an epoxy, polyester thermosetting plastic, etc. Fibre-reinforced plastics are a category of composite plastics that specifically use fibre materials to mechanically enhance the strength and elasticity of plastics. The original plastic material without fibre reinforcement is known as the matrix.

Photopolymer

A **photopolymer** is a polymer that changes its properties when exposed to light, often in the ultraviolet or visible region of the electromagnetic spectrum. Hardening of the material occurs as a result of cross-linking when exposed to light. Photopolymers undergo a process called Curing where oligomers are cross-linked upon exposure to light, forming what is known as a network polymer. The result of photo curing is the formation of a thermoset network of polymers.

Epoxy

Epoxy resins may be reacted (cross-linked) either with themselves through catalytic homopolymerisation, or with a wide range of co-reactants including polyfunctional amines, acids and their anhydrides, phenols, and alcohols. These co-reactants are often referred to as hardeners or curatives, and the cross-linking reaction is commonly referred to as curing. Epoxy takes about 24 to 48 hours for effective curing. In the aerospace industry, epoxy is used as a structural matrix material which is then reinforced by fibre.

Glass Fibre Reinforcements

Glass fibre is a material consisting of numerous extremely fine fibres of glass. It is not as strong or as rigid as carbon fibre but is much cheaper and significantly less brittle when used in composites. Hence Glass fibres are used as a reinforcing agent for many polymer products; to form a very strong and relatively lightweight fibre-reinforced polymer (FRP) composite material.

Hand Lay Up Process

Hand lay-up technique is the simplest method of composite processing. Thin plastic sheets are used at the top and bottom of the mould plate to get good surface finish of the product. Reinforcement in the form of woven mats or chopped strand mats are cut as per the mould size and placed at the surface of mould after Perspex sheet. Then thermosetting polymer in liquid form is mixed thoroughly in suitable proportion with a prescribed hardener (curing agent) and poured onto the surface of mat already placed in the mould. The polymer is uniformly spread with the help of brush. The process is repeated for each layer of polymer and mat, till the required layers are stacked. After placing the plastic sheet, release gel is sprayed on the inner surface of the top mould plate which is then kept on the stacked layers and the pressure is applied. After curing either at room temperature or at some specific temperature, mould is opened and the developed composite part is taken out and further processed.

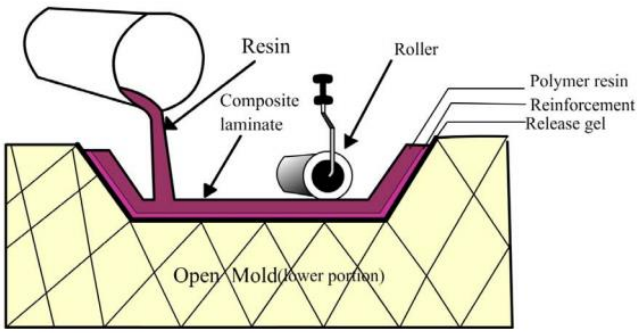

Figure 17 Hand Layup Method [D]

Fabrication Process of Photopolymer Matrix with Glass Fibre Reinforcement

1. Preparation of Mould using double sided tape and overhead projection sheet.

2. Pour photopolymer resin to form a layer (Layer 1).

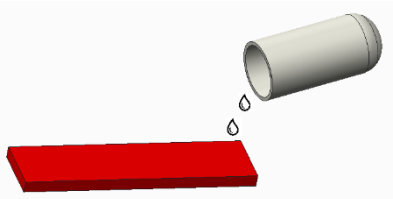

3. Curing of photopolymer layer (using UV light) for 5 minutes.

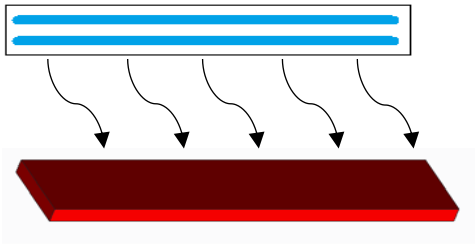

4. Place a layer of glass fibre over the photopolymer layer.

5. Place 2 wires of Nitinol on the layer and keep the wires taut by applying external tension.

6. Apply 1 more alternative layers of photopolymer and glass fibres and the plate is cured from both the sides.

7. Plate is removed from the mould and hardened using hardener.

10cm x 3cm

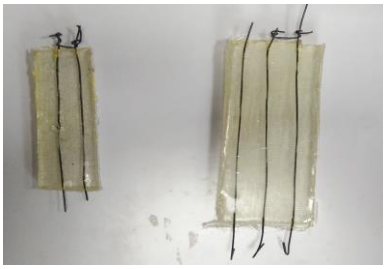

15cm x 5cm

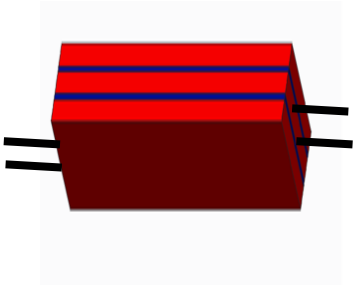

Figure 18 Photopolymer Structure

Fabrication Process of Epoxy Matrix with Glass Fibre Reinforcement

1. Preparation of Mould using double sided tape, overhead projection sheet, and wires clamps.

2. Place the wire in the setup and clamp them in tension.

3. Preparation of epoxy hardener mixture where epoxy is mixed with hardener in the ratio 10:3.

4. Apply a layer of epoxy mixture using hand layup process and place a layer of glass fibre reinforcement on it.

5. Apply more alternative layers of epoxy mixture and glass fibres to get the epoxy blade of required thickness.

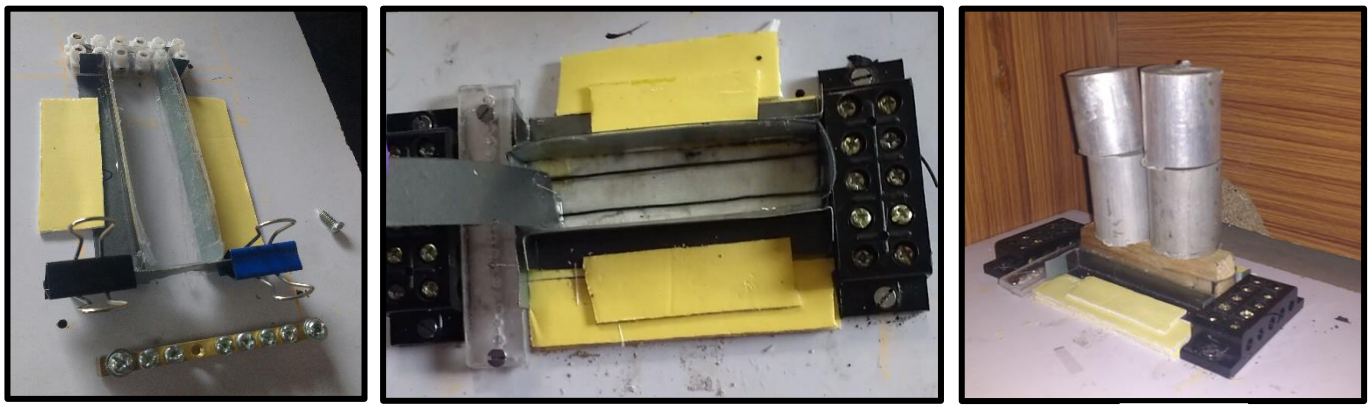

(a) *(b)* *(c)*

Figure 19 Steps involved in Blade fabrication. (a) Preparation of Mould (b) SMA wires are fixed and epoxy has been placed (c) Curing of resin

6. Apply sufficient weights on the fixture to keep the wires taut during curing process. Allow the mixture to cure for 24 hours.

7. Take out the weights and separate the clamps to get the SMA embedded epoxy plate.

4.4 DEFLECTION ANALYSIS OF SMART PLATES

1. SMA embedded photopolymer plates

The deflection analysis was performed by using the Laser Displacement Sensor (LDS). Laser displacement sensor uses the triangulation method to measure the displacement. The composite plate is fixed in the cantilever setup and the vertical deflection of the blade is measured by the LDS.

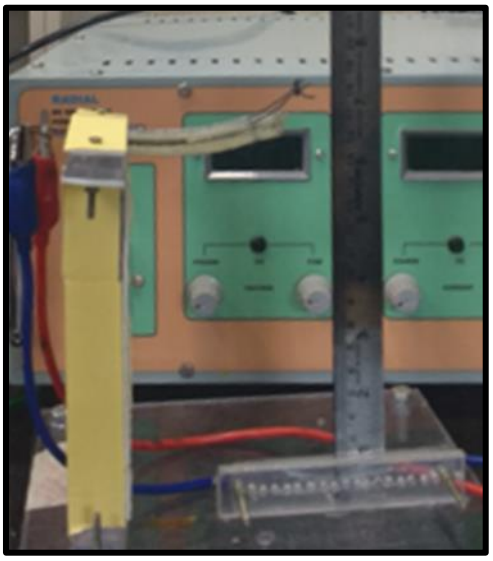

Figure 20 Deflection analysis of Photopolymer structure

In photo polymeric smart plates, the stiffness is less and hence more deflection can be achieved on heating. The maximum deflection of 10 mm was achieved for a 10 mm thick plate with 2 layers of glass fibre reinforcement on joule heating .The blade was, however, unable to come back to its initial position due to less elastic force. Photopolymers in the vicinity of SMA wires melts on heating and thus leave the wires. SMA wire loosen up on repetitive heating and hence the fatigue life is less for photopolymers. Photopolymer cannot be used for wind turbine blades as it has very less stiffness and it shows very less fatigue life.

2. SMA embedded epoxy plates

Figure 21 Deflection analysis of Epoxy structure

In epoxy smart plates, the stiffness is high as compared to photopolymer and provides higher recovery stress. The epoxy plates are able to come back to its initial position and show 2 way shape memory effect. Epoxy has higher melting point and does not melt with the heat dissipated in the vicinity of the SMA wires.

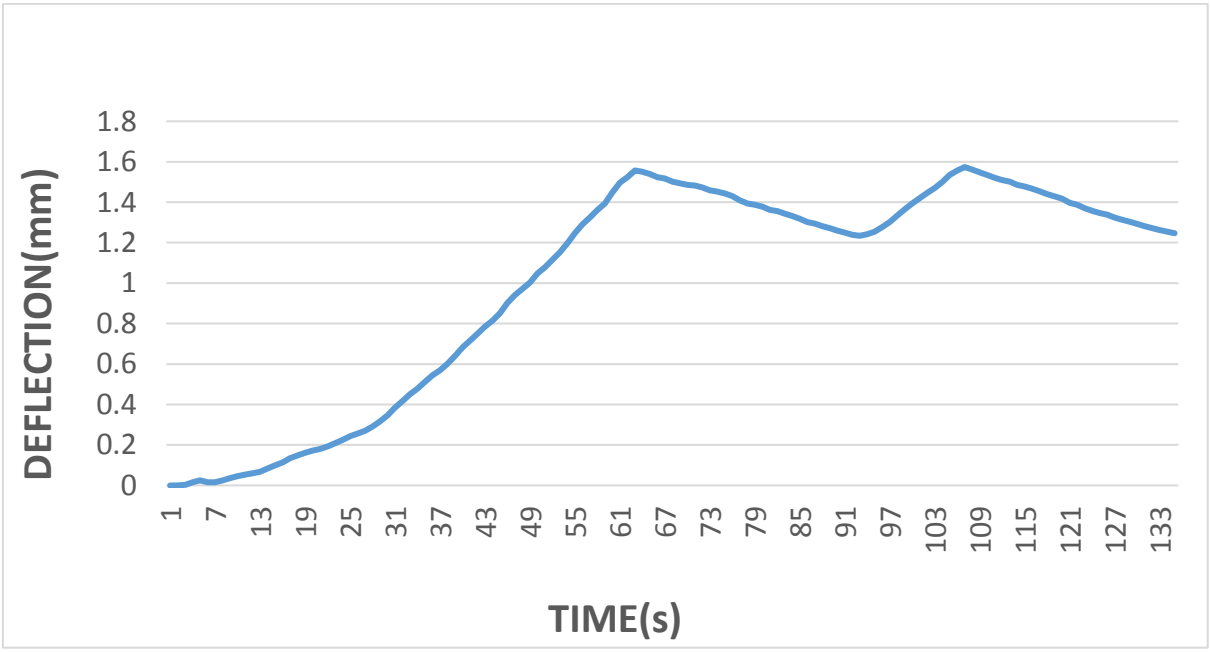

Figure 22 Repeated heating and cooling cycles over time

4.5 MOULD PREPARATION OF WIND TURBINE BLADES

Wind turbine blade is manufactured by applying epoxy composites on the blade mould which is then cured. The cardboard mould for the blade model was developed using wax pattern. The wax pattern was built with aerofoil profile.

Figure 24 Cardboard mould for Wax pattern

Figure 24 Wax Pattern

4.6 FABRICATION OF SMART BLADES

1. Fabrication of SMA spring embedded blade

1. The cardboard mould is prepared and overhead projection sheets are applied on the inner surface of the mould to get good surface finish.
2. Epoxy is mixed thoroughly in 10:3 ratio with hardener and placed on the mould by Hand Lay-up Method. On the layer of epoxy, a layer of glass fibre reinforcement is applied.
3. The process is repeated, till the required layers are stacked.
4. After curing at room temperature mould is opened .For epoxy based system, normal curing time at room temperature is 24-48 hours.
5. On curing, holes are drilled in the blade and spring is connected across them using fasteners.

Figure 26 Curing of Smart blade

Figure 26 Blade produced

2. Fabrication of SMA wire embedded blade

1. The cardboard mould is prepared and overhead projection sheets are applied on the outer surface of the mould to get good surface finish.

2. The SMA wires are placed on the mould and tighten using clamps to prevent wire misalignment during curing.

3. Epoxy is mixed thoroughly in 10:3 ratio with hardener and placed on the mould by Hand Lay-up Method. On the layer of epoxy, a layer of glass fibre reinforcement is applied.

4. The process is repeated, till the required layers are stacked. After curing at room temperature mould is opened .For epoxy based system, normal curing time at room temperature is 24-48 hours.

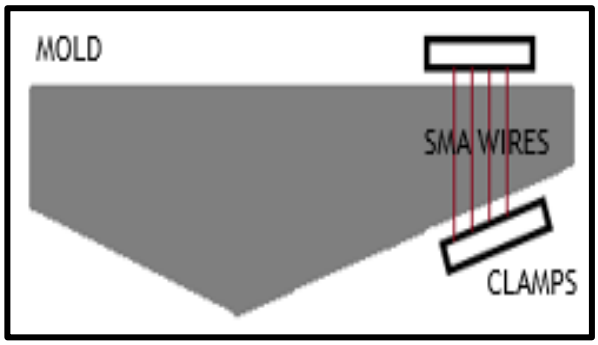

Figure 28 Schematic diagram of SMA embedded blade casting

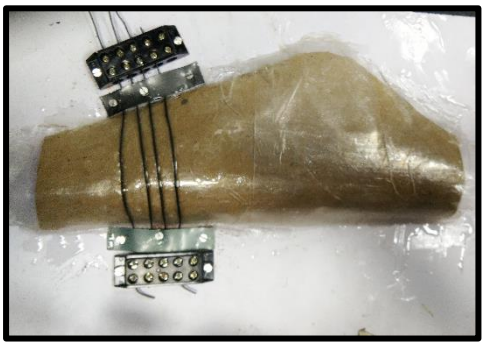

Figure 28 SMA embedded blade casting

CASTING SETUP

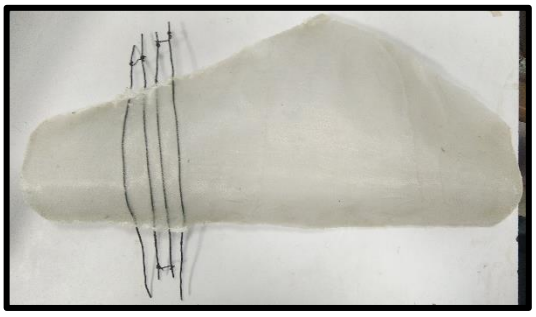

Figure 29 Prepared Blade

The produced blades has some defects in it like presence of air bubbles, bad finishing , improper orientation of SMA wires which reduced the strength of the composite blade. The uneven pressure applied to the mould due to airfoil contour lead to variable thickness of the blade model.

4.7 DEFLECTION ANALYSIS OF SMART BLADES

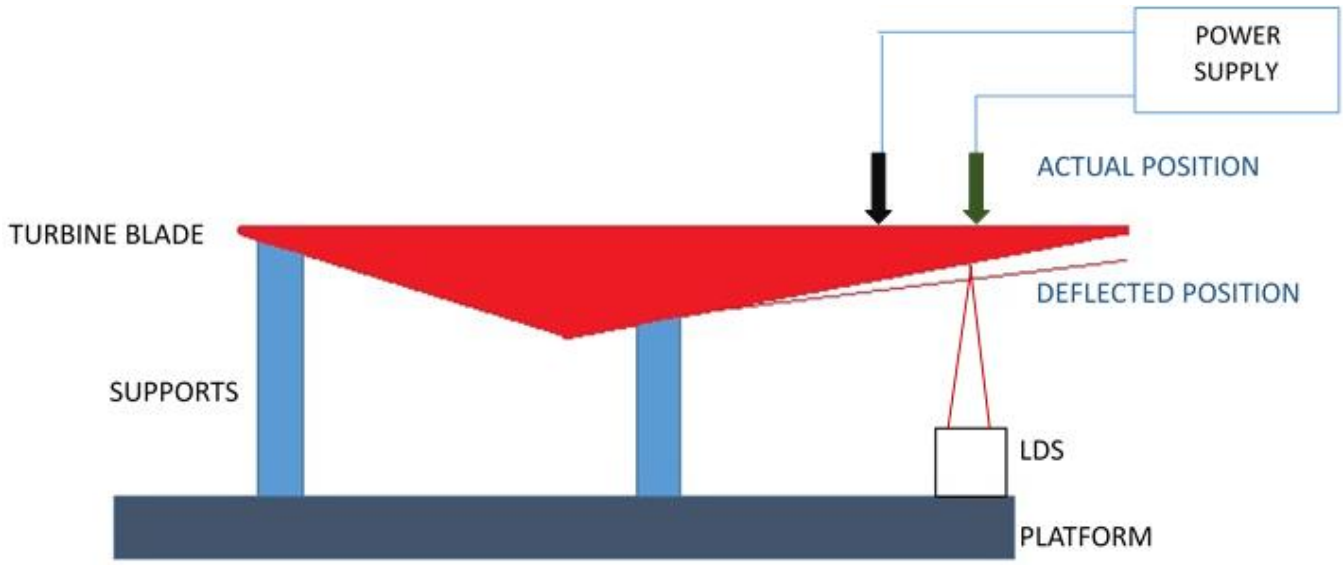

Figure 30 Schematic diagram of Experimental Setup

The deflection analysis was performed by using the Laser Displacement Sensor. Laser displacement sensor uses the triangulation method to measure the displacement. The composite blade is fixed in the cantilever setup and the vertical deflection of the blade is measured by the LDS. The actuation is achieved by Joule Heating. When the nitinol wires are heated, they acquire the trained shape and the blade changes its airfoil shape. As the blade changes its airfoil shape, there is a deflection in trailing edge. The angle of deflection of trailing edge can also be measured.

Actuation through Joules Heating

WITH SPRING

Voltage = 5 volts

Wire diameter = 770 µm

No. of turns = 18

Figure 31 SMA Spring actuated Blade

WITH WIRES

Voltage = 12 volts

Wire diameter = 1.5 mm

Length = 27 cm

Figure 32 SMA Wire actuated Blade

ELECTRICAL RESISTIVITY of SMA wire:

Austenite - 82*10e-6 Ω·cm Martensite - 76*10e-6 Ω·cm

4.8 DISPLACEMENT V/S TIME GRAPHS (SMA SPRING EMBEDDED BLADE)

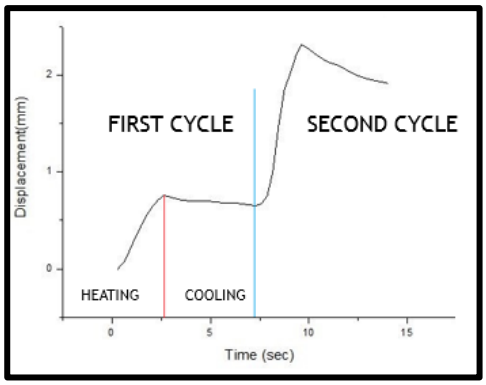

Voltage = 5 V

Heating time =2 sec

Cooling time = 5 sec

No. of cycles=2

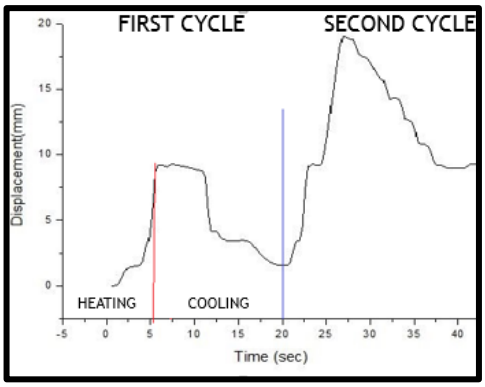

Voltage = 5 V

Heating time = 5 sec

Cooling time = 15 sec

No. of cycles=2

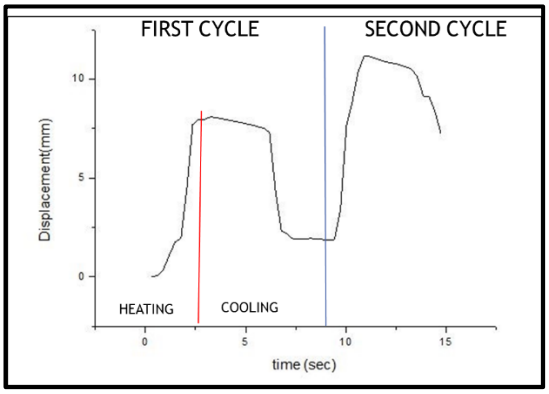

Voltage = 5 V

Heating time = 3 sec

Cooling time = 10 sec

No. of cycles=2

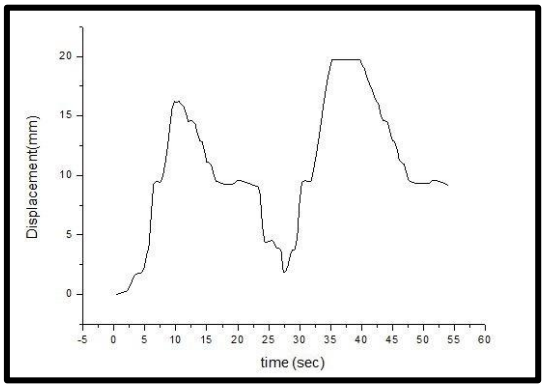

Voltage = 5 V

Heating time = 7 sec

Cooling time = 20 sec

No. of cycles=2

Maximum deflection obtained = 20.9 mm **Angle of deflection = 15 deg**

CHAPTER 5: COMPUTATIONAL FLUID DYNAMICS (CFD)

Computational fluid dynamics (CFD) is a branch of fluid mechanics that uses numerical analysis and algorithms to solve and analyse problems that involve fluid flows. CFD is the use of applied mathematics, physics and computational software to visualize how a gas or liquid flows -- as well as how the gas or liquid affects objects as it flows past. Computational fluid dynamics is based on the Navier - Stokes equations. These equations describe how the velocity, pressure, temperature, and density of a moving fluid are related.

Numerical simulations of fluid flow (will) enable -

- architects to design comfortable and safe living environments
- designers of vehicles to improve the aerodynamic characteristics
- chemical engineers to maximize the yield from their equipment
- petroleum engineers to devise optimal oil recovery strategies

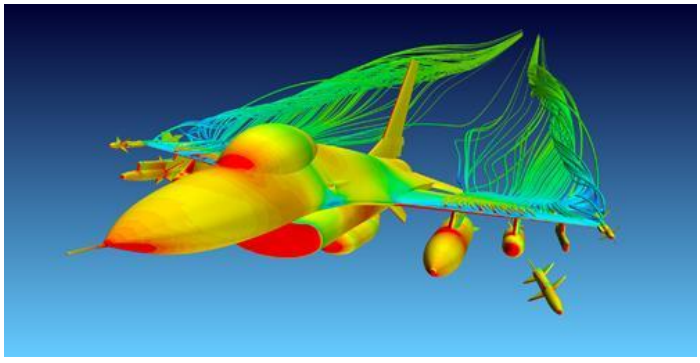

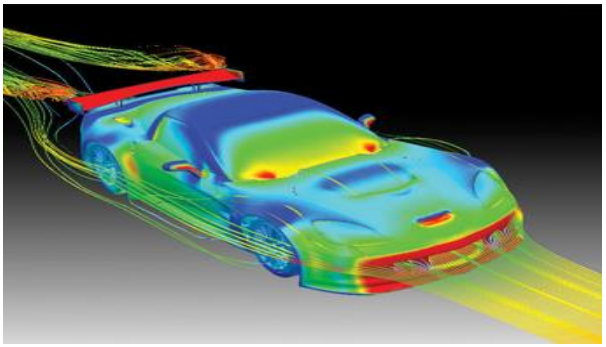

Figure 33 Examples of CFD Applications [E]

5.1 The Need for CFD

Applying the fundamental laws of mechanics to a fluid gives the governing equations for a fluid. The conservation of mass equation is

$$\frac{\partial \rho}{\partial t} + \nabla \cdot (\rho \vec{V}) = 0$$

And the conservation of momentum equation is

$$\rho \frac{\partial \vec{V}}{\partial t} + \rho(\vec{V} \cdot \nabla)\vec{V} = -\nabla p + \rho \vec{g} + \nabla \cdot \tau_{ij}$$

Where

- ρ is the density,
- V is the flow velocity,
- ∇ is the Del operator.
- p is the pressure
- τij is the deviatoric stress tensor, which has order two,
- g represents body accelerations (per unit mass).

These equations along with the conservation of energy equation form a set of coupled, nonlinear partial differential equations. It is not possible to solve these equations analytically for most engineering problems. However, it is possible to obtain approximate computer-based solutions to the governing equations for a variety of engineering problems. This is the subject matter of Computational Fluid Dynamics (CFD).

5.2 The Strategy of CFD

Broadly, the strategy of CFD is to replace the continuous problem domain with a discrete domain using a grid. In the continuous domain, each flow variable is defined at every point in the domain. For instance, the pressure p in the continuous 1D domain shown in the figure below would be given as

$$p = p(x), \quad 0 < x < 1$$

In the discrete domain, each flow variable is defined only at the grid points. So, in the discrete domain shown below, the pressure would be defined only at the N grid points.

$$p_i = p(x_i), \quad i = 1, 2, \ldots, N$$

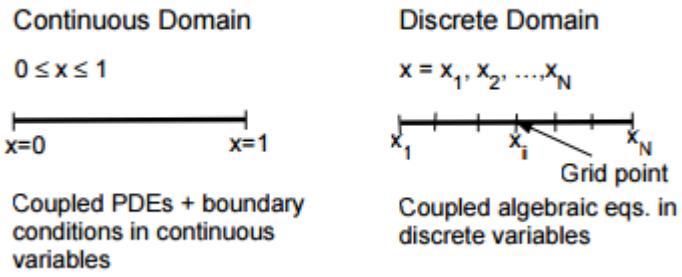

In a CFD solution, one would directly solve for the relevant flow variables only at the grid points. The values at other locations are determined by interpolating the values at the grid points. The governing partial differential equations and boundary conditions are defined in terms of the continuous variables p, V etc. One can approximate these in the discrete domain in terms of the discrete variables p_i , V_i etc. The discrete system is a large set of coupled, algebraic equations in the discrete variables. Setting up the discrete system and solving it (which is a matrix inversion problem) involves a very large number of repetitive calculations, a task we humans palm over to the digital computer.

5.3 ANSYS Fluent

In the present case, the detailed explanations and studies regarding the lift, drag, and the variation in trailing edge angle that occurs in an aerofoil is simulated using the ANSYS FLUENT software. So in order to deal with these scenarios we used the GAMBIT software to develop initially the two dimensional structure of an aerofoil and mesh it accordingly to obtain the rigorously accurate calculations.

The ANSYS FLUENT software is computational fluid dynamic software that investigates thoroughly on an aerodynamic structure like the aerofoil, rather than any experimental method. Using this software had already altered our perspective regarding the aerofoil. The study of the aerofoil using the ANSYS FLUENT software made it clear about the drag force, lift force, coefficient of drag and coefficient of lift. Various trailing edge angle such as 0°, 5°, 10° and 15° were simulated and analyzed. From the iterations that we have undertaken, we understood a general trend about how the various parameters change in accordance with varying trailing edge angle.

5.4 Problem and Inputs

The problem is to calculate lift force at different wind speed when wind flows around airfoil NACA 4412 at 0°, 5°, 10° and 15° trailing edge angles. And also generate pressure contour, velocity vector, Graphs of coefficient of drag and coefficient of lift diagram for the airfoil without any deflection. For that, we take some initial inputs and boundary condition for our problem which are shown in the table.

No	Input	Value
1	Velocity of flow	0 to 150 m/s
2	Operating Temperature	300 K
3	Operating Pressure	101325 kPa
4	Fluid	air
5	Density of Fluid	1.225 kg/m3
6	Length	1m
7	Trailing Edge Angle	0°,5°,10° and 15°

Table 1 Input Parameters

5.5 Geometry

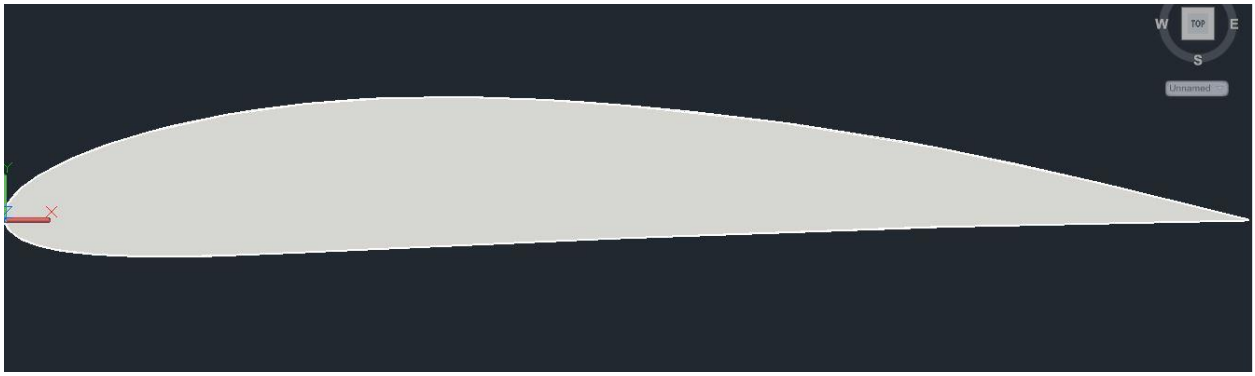

No deflection

5° Trailing Edge angle

10° Trailing Edge angle

15° Trailing Edge angle

5.6 Meshing

The meshing of aerofoil profile was also done in ANSYS. This meshing process and principles are based on the theory of finite element analysis method. The final meshed geometry surrounding the airfoil is as shown in the following figure.

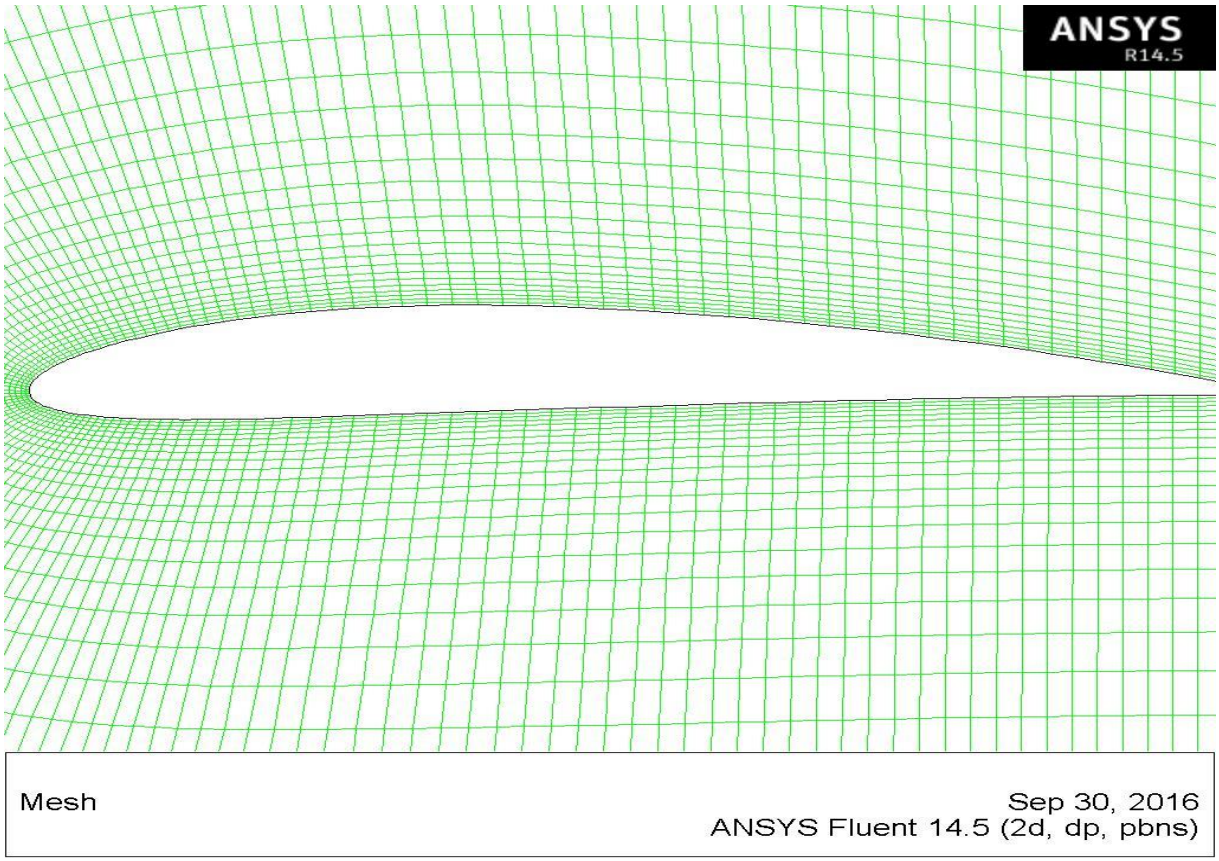

Figure 34 Final meshed region surrounding the aerofoil geometry

5.7 Results and Discussions

For 0° trailing edge angle, we obtain following pressure contour and velocity vector diagram

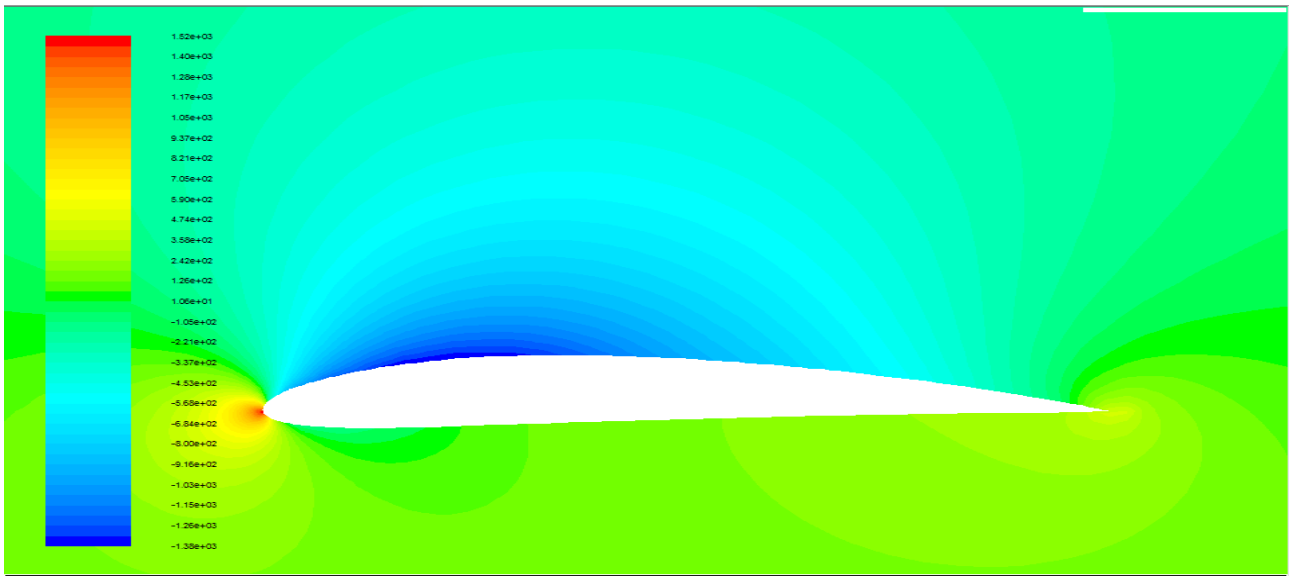

Figure 35 Contours of static pressure at 1.2° angle of attack

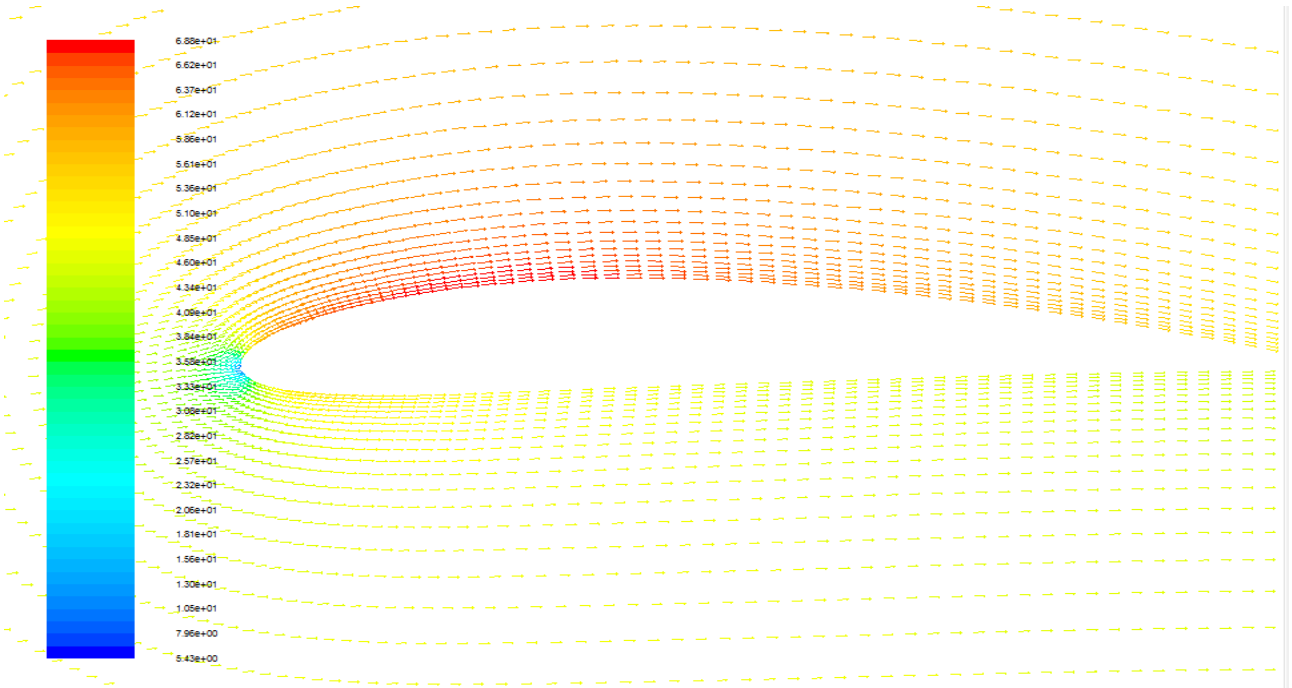

Figure 36 Velocity vector at 1.2° angle of attack

The velocity on the upper surface of the airfoil has a higher value than the lower surface. Thus the pressure at the upper surface is low compared with the lower surface of aerofoil. According to Bernoulli's theorem, the object will move from higher pressure region to lower pressure region. **Thus the lift occurs in airfoil**.

Graphs of coefficient of drag and coefficient of lift at AOA 1.2° verses number of iterations is shown below

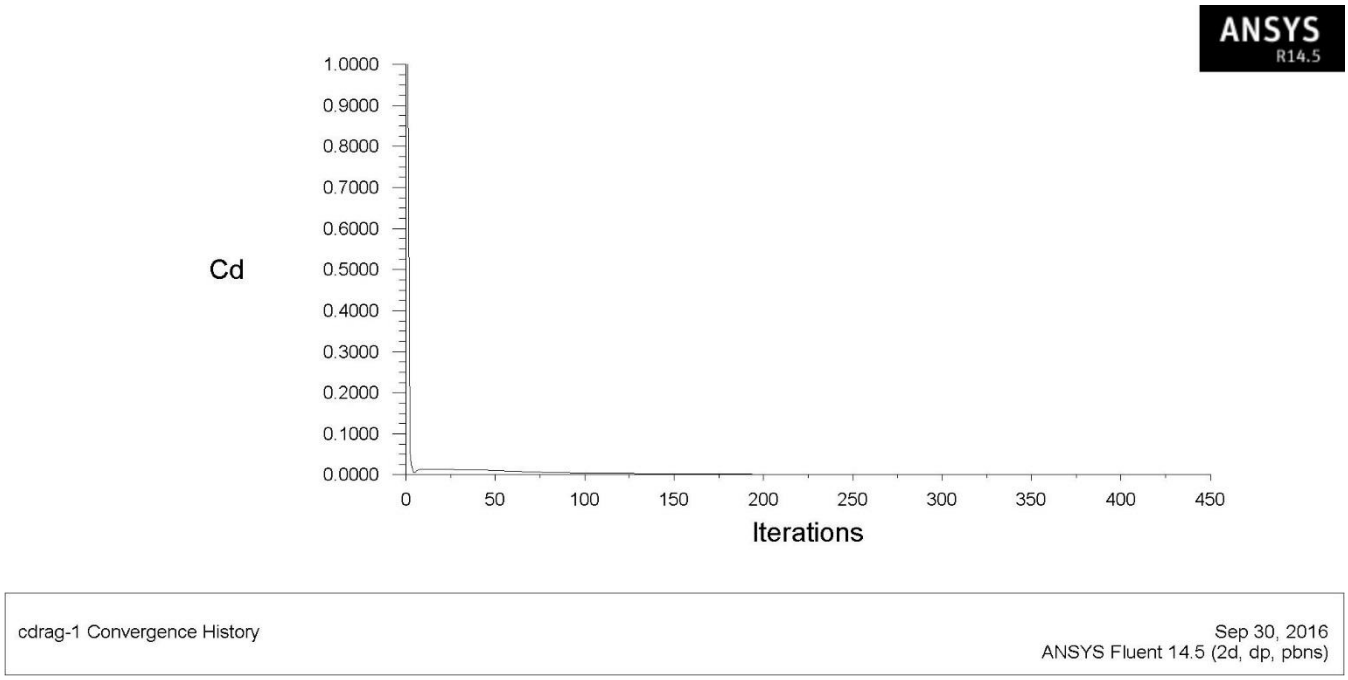

Figure 37 Graph of coefficient of drag at 1.2° of AOA

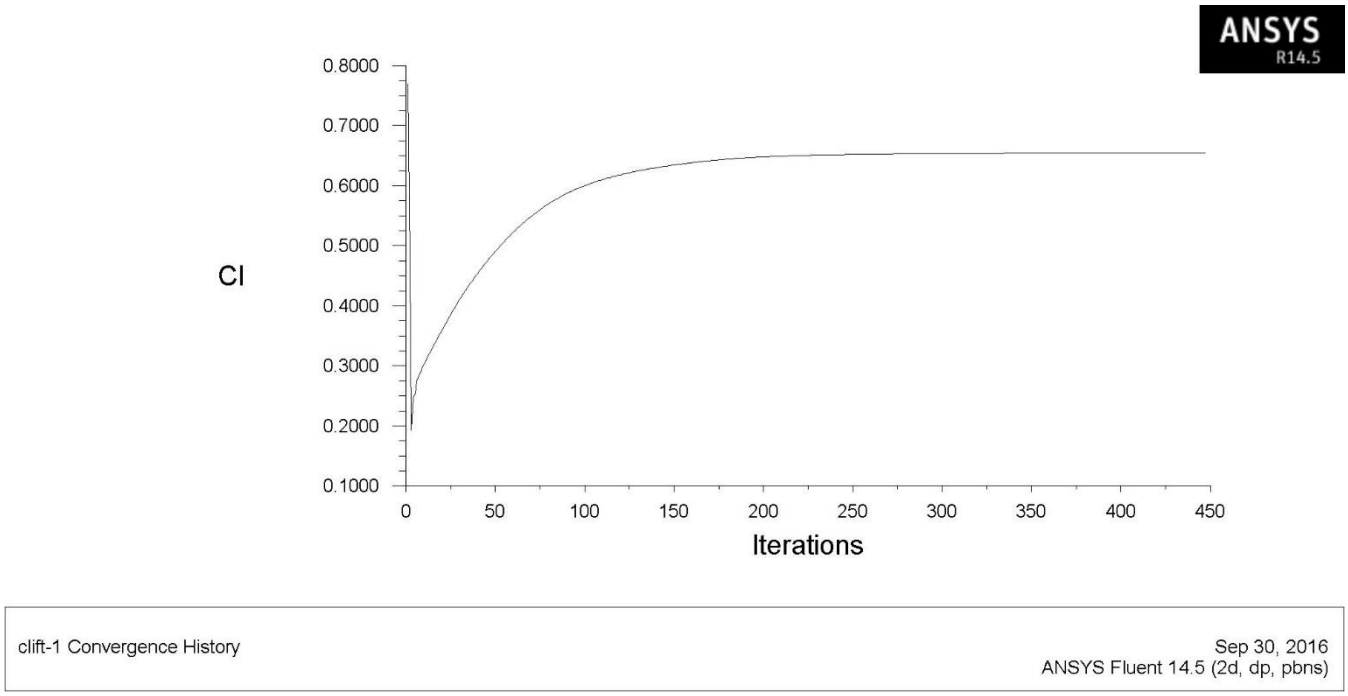

Figure 5 Graph of coefficient of lift at 1.2° of AOA

The value of coefficient of drag is 1.0693e-03

The value of coefficient of lift is 0.654.

Here the lift force is plotted against different wind speed at different trailing edge angle.

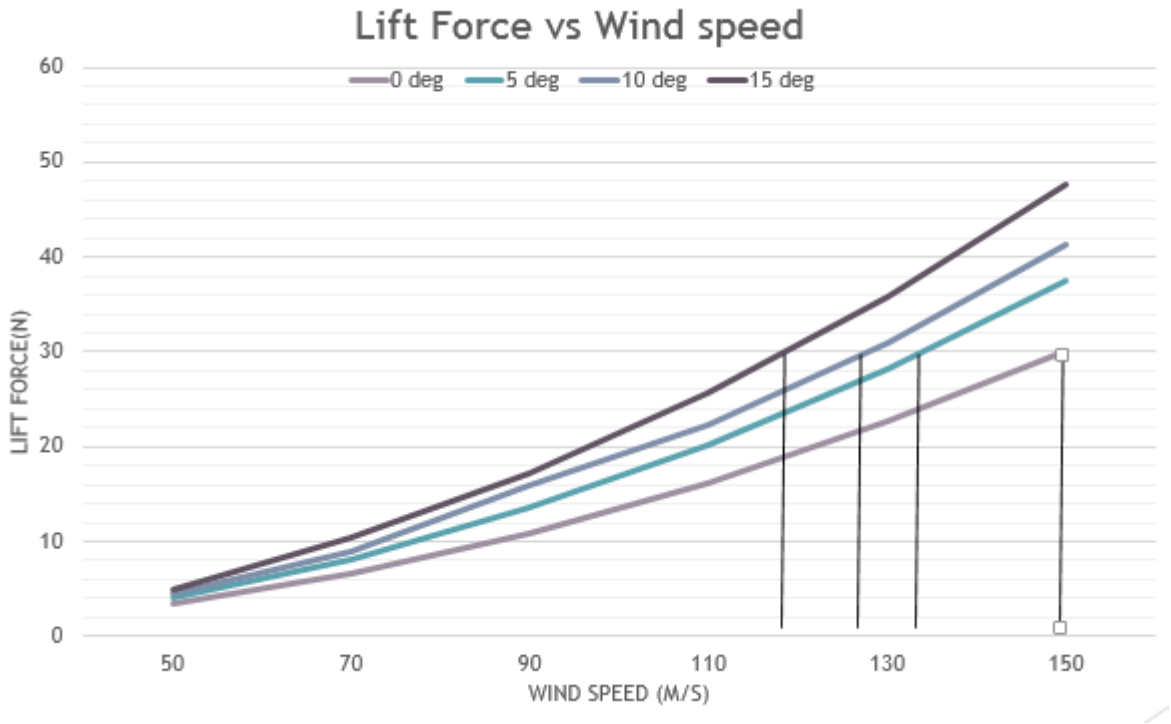

Figure 38 Lift V/S Wind Speeds

Observations

The CFD analysis gives a clear understanding of the flow around the airfoil. This method is simpler, cost effective and reliable. The meshing is a very important phase in the development of CFD analysis. The result depends on the size of mesh created. Greater the meshed cells, higher are the accuracy of the result. Careful meshing is must in CFD as it is a balance between computation time and accuracy.The purpose of this simulation was to compare the different values of lift force obtained by changing the angles of trailing edge of NACA 4412 airfoil. Also to see the variation in static pressure and Velocity vector. It is obvious that there were significant changes in lift force when the angle of trailing edge of the airfoil was changed.

CHAPTER 6:

CONCLUSIONS

- SMA smart blades are technically feasible and better than conventional complex mechanisms like motors, hydraulic etc. for getting deflection.
- Efficiency of the blade can be increased that is more power output for the same wind speed.
- Rotor energy capture can be increased, the fatigue load will be reduced thereby increasing the component lifetimes, lesser maintenance requirements and overall lower costs.
- Maximum deflection achieved with wire embedded blade is 13.1 mm.
- Maximum deflection achieved with spring actuated blade is 20.9 mm.

FUTURE WORK

- Design a robust controller to control the actuation of trailing edge of smart blade according to the wind dynamics.
- Tests have to be performed for large number of cycles (around 1000-1500) to determine the fatigue behaviour.
- Wind tunnel testing of the smart blade to test its performance in practical situations.
- Comparison of the results of wind tunnel testing with the CFD analysis.

References

[1]Min-Woo Han, Hugo Rodrigue: Woven type smart soft composite for soft morphing car spoiler

[2]Stephen Daynes and Paul M Weaver: A morphing trailing edge device for a wind turbine

[3] Hugo Rodrigue, Wei Wang, Binayak Bhandari, Min-Woo Han, and Sung-Hoon Ahn: Cross-Shaped Twisting Structure Using SMA-Based Smart Soft Composite

[4] Min-Woo Han, Hugo Rodrigue, Hyung-Il Kim, Sung-Hyuk Song, Sung-Hoon Ahn: Shape memory alloy/glass fibre woven composite for soft morphing winglets of unmanned aerial vehicles

[5]Wang W, Rodrigue H, Ahn S-H: Smart soft composite actuator with shape retention capability using embedded fusible alloy structures

[6]Van Humbeeck J.: Shape memory alloys: a material and a technology

[7] Danish Wind Industry Association

[8] Paul Cantrell: http://www.copters.com/aero/airfoils.html

[9] The Electropaedia: http://www.mpoweruk.com/

[10] NPTEL: http://nptel.ac.in/courses/112107085/module5/

[11] Pratt Miller: http://prattmiller.com/contentimagedata/